RESEARCH ARTICLE | OCTOBER 26 2020

# Photoanode nanostructure optimization in dye-sensitized solar cell

Ro'sil Qohhar; Edy Supriyanto ✉; Sujito; Agung Tjahjo Nugroho; Agus Subekti



*AIP Conf. Proc.* 2278, 020035 (2020)
https://doi.org/10.1063/5.0015224

# Photoanode Nanostructure Optimization in Dye-Sensitized Solar Cell

Ro'sil Qohhar[1], Edy Supriyanto[2,a)], Sujito[3], Agung Tjahjo Nugroho[4], Agus Subekti[5,]

[1,2,3,4,5]*Physics Departement, Faculty of Mathematics and Natural Sciences, Jember University, Jl. Kalimantan No. 37, Jember 68121, Indonesia*

[a)]Corresponding author: edysupriyanto@unej.ac.id

**Abstract.** The rapid development of industries that use fossil fuels produces negative impacts on the environment. For the first time in human history, $CO_2$ levels in the atmosphere have doubled compared to the ice age. Renewable energy is one solution to reduce dependence on fossil fuels. One source of renewable energy is solar energy. This energy can be utilized using the Dye-Sensitized Solar Cell. DSSC is environmentally friendly, low cost, and can be grown on elastic thin films. DSSC consists of four main components, one of which is photoanode. Photoanode serves as a medium for photogeneration of electrons to produce an electric current. For better performance, DSSC was analytically modeled by several previous researchers. But only on macro parameters such as working temperature, solar intensity, and electron lifetime. It is necessary to make variations on the photoanode semiconductor material and nanostructure parameters to optimize DSSC performance. There are three best variations in a photoanode semiconductor material such as $TiO_2$, ZnO, $Nb_2O_3$. Further modeling of nanostructures photoanode constituent particles uses the constant overlap method. This modeling can describe nanostructural parameters such as diffusion coefficient, absorption coefficient, and porosity to describe J-V characteristics of DSSC. The simulation is done after the modeling results agreed well with the experimental results based on the reference. Simulation results illustrate the value of sunlight penetration depth that affects the short circuit current density. The short circuit current is proportional to the absorption coefficient and the diffusion coefficient. 0.41 porosity is the optimum value that produces maximum power. Photoanode semiconductor material based on the J-V characteristics of the best is $TiO_2$, ZnO, $Nb_2O_3$.



## INTRODUCTION

The rapid development of industrial activities lately has resulted in a decrease in the quality of the environment. This is due to the increase in hazardous organic waste produced by the industry. One of them is an increase in $CO_2$ levels. The Mauna Loa Observatory in Hawaii, notes that the concentration of $CO_2$ in the atmosphere has crossed the climate threshold for the first time in human history. $CO_2$ levels have reached 415 per million parts (ppm) [1]. Even before modern humans existed, Earth had never experienced a surge in $CO_2$ levels that high. During the ice age, the level of carbon dioxide in the atmosphere was around 200 ppm. Moreover, burning fossil fuels worsens the condition. This causes the increasing release of carbon dioxide and other greenhouse gases. This makes more heat trapped on Earth and increases global temperatures. So far, the world's temperature has risen by around 1 degree Celsius.

World energy consumption in 2015 reached 18.5 TW. Even in 2050, energy requirements will double to 30 TW as the population and industry increase [2]. Non-fossil energy development continues to be encouraged, such as wind, water, biomass, geothermal, and solar energy. Solar cells lead efforts in meeting energy capacity, and they are considered a competitive source of energy. Solar energy can supply up to 23000 TW every year. Clean and environmentally friendly energy is available every day and can meet the energy needs of mankind with only less than one hour of exposure [3]. ASEAN has the advantage of geographical location for the utilization of solar cells because the sun shines throughout the year.

*Climate Change and Sustainability Engineering in ASEAN 2019*
AIP Conf. Proc. 2278, 020035-1–020035-9; https://doi.org/10.1063/5.0015224
Published by AIP Publishing. 978-0-7354-4008-1/$30.00

Dye-Sensitized Solar Cell (DSSC) is one of the third-generation solar cells. The advantage of DSSC is that it can be grown on a thin layer of conductor plastic, and it can be used in dim light conditions. DSSC consists of four main components, including photoanode, dye, electrolyte, and counter electrode [4]. Fotoanoda plays two roles in dye adsorption and electron transport media. Photoanode is grown on the surface of Transparent Conducting Oxide (TCO) which is mesoporous semiconductor metal-oxide nanoparticles. Generally used semiconductor ZnO, $TiO_2$, $Nb_2O_5$. Titanium dioxide semiconductors ($TiO_2$) are used because they are inert chemically and biologically, non-toxic, and inexpensive [5]. Zinc oxide (ZnO) was the closest alternative to $TiO_2$ as a semiconductor material in DSSC. $TiO_2$ and ZnO have almost the same bandgap energy and the same electron affinity. ZnO has a much higher diffusivity of electrons than $TiO_2$, high electron mobility, large excitation binding energy, available at low prices, and stable against photo corrosion [6]. The next material, niobium pentoxide received attention in the scope of DSSC research because it can be applied to anode or cathode cells. $Nb_2O_5$ can also act as a barrier layer that is very good at reducing electron loss due to recombination with electrolytes [2].

The problem on this paper is low efficiency on DSSC. It has an efficiency up to 3% but further improvements are needed for better performance. Previous research already modeling $TiO_2$ photoanode with some internal parameters [7]. Characteristics of current density and voltage of DSSC are influenced by internal parameters such as thickness, work temperature, ideal factors, and light intensity. But it still needs to be done variations for nanostructural parameters as well as variations in the photoanode semiconductor material. Nanostructural parameter play an important role because the amount of dye that can be adsorp on photoanode particles ($CN$) depends on its porosity ($p$). The purpose of this paper is to optimize DSSC using photoanoda nano particle intersection modeling. It can describe nano structure parameters effect from DSSCs such as photoanode porosity, absorption coefficient, and diffusion coefficient to $J-V$ characteristic.

## EXPERIMENTAL DETAIL

In a DSSCsteady-state condition, diffusion derivative equations can describe injected electrons from dye molecules, transport in photoanodes and recombination with electrolytes on the surface can be described using [8]

$$D\frac{\partial^2 n(x)}{\partial x^2}-\frac{n(x)-n_0}{\tau}+\Phi\alpha e^{-\alpha x}=0 \tag{1}$$

with $D$ is the electron diffusion coefficient; $n(x)$ is excess electrons concentration in $x$; $x$ is coordinates of the surface of TCO; $\tau$ is the free-electron lifetime of conduction band; $n_0$ Is electron concentration in dark conditions; $\Phi$ is light intensity, and $\alpha$ is the photoanode light absorption coefficient. When short circuit, there are no electrons that reach the electrode counter directly, and the electron is equal to the light-current. There are two boundary conditions

$$n(0)=n_0 \tag{2}$$

$$\left.\frac{dn}{dx}\right|_{x=d}=0 \tag{3}$$

with $d$ is photoanode thickness. Short circuit current density becomes

$$J_{sc}=\frac{q\Phi L\alpha}{1-L^2\alpha^2}\left[-L\alpha+\tanh\left(\frac{d}{L}\right)+\frac{L\alpha\exp(-d\alpha)}{\cosh\left(\frac{d}{L}\right)}\right] \tag{4}$$

where $L$ is electron diffusion length which is the result of $\sqrt{D\tau}$ and $q$ is an electron charge.

If the DSSC works on a potential difference $V$ between the electrolyte reduction potential and the Fermi level of photoanode, electrons density on the surface $x=0$ increase to $n$ according to the first boundary conditions,

$$n(0)=n \tag{5}$$

The second boundary condition on $x = d$ does not change according to the eq. (3). Then, the relationship between $J$ and $V$ written after obtaining the equation solution (1):

$$V = \frac{kTm}{q} \ln \left[ \frac{L(J_{sc} - J)}{qDn_0 \tanh\left(\frac{d}{L}\right)} + 1 \right] \tag{6}$$

With $k$ Boltzman, constant, and $m$ is the ideal factor [9]; [10]. Eq. (6) has been validated by Soedergren et al. in previous research [8]. While the output power of a DSSC can be written.

$$P = JV = \frac{JkTm}{q} \ln \left[ \frac{L(J_{sc} - J)}{qDn_0 \tanh\left(\frac{d}{L}\right)} + 1 \right] \tag{7}$$

In order to optimize the performance of a photoanode nanostructure, porosity parameters play an important role. Internal parameters of porosity $p$ related to the internal surface area and the dye-sensitized nano-$TiO_2$ coordinates that impact on $\alpha$ and $D$ like eq. (4). In DSSC fabrication, $p$ can be adjusted by adjusting the amount of polyethylene glycol (PEG), which is added to the electrode preparation process [11]. In fact, effective porosity between 0.4 and 0.7 can be produced through a short sintering process (30 minutes) [12]. The longer the sintering process results in reduced electrode porosity. This phenomenon is reviewed with high and low porosity conditions that are modeled by the constant overlap method.

The first step in modeling a photoanode nanostructure by assuming that all nanoparticles are uniform with a spherical shape and a radius of 10 nm [13]. The physical overlap between the two particles is depicted in FIGURE 1.

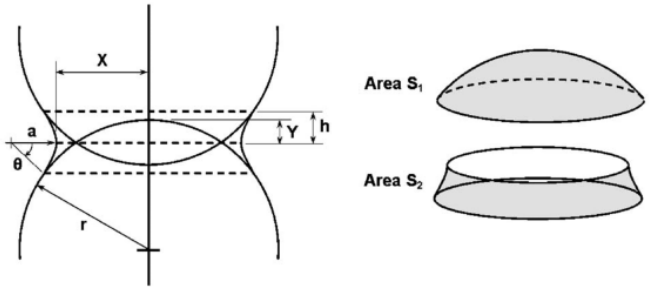


**FIGURE 1**. Illustration of connection on the overlap of two nanoparticles

Relationships based on geometric parameters can be written [14]:

$$x = \left[ \frac{4rY^2(3r - Y)}{3} \right]^{1/4} \tag{8}$$

$$S_1 = 2\pi r(h + Y) = 2\pi r \left[ \frac{X^2(r - Y)}{4r^2 + X^2} + Y \right] \tag{9}$$

$$S_2 = 2\pi Xa\theta = 2\pi \frac{X^3}{4r} \arcsin \left[ \frac{4r(r - Y)}{4r^2 + X^2} \right] \tag{10}$$

where $X$ neck surface radius; $r$ nanoparticle radius; $Y$ overlap; $S_1$ and $S_2$ is the original and new surface area of the overlap zone of a nanoparticle. A total number of particles $N$ and coordination numbers $CN$ effect on $p$ [11]. Enhancement $CN$ reduce $p$. This study explains the maximum meeting package with $CN = 6$, porosity 0,41. Value $p$ it is then used as a transition point like the lower limit ($p \geq 0{,}41$) pada constant overlap method. Relationship between $\alpha$ and $p$ can be derived based on the total surface area of the dye-sensitized photoanode particles. Here's the relationship between $\alpha$ and $p$ [15]:

$$S = N(4\pi r^2 - CN\, \Delta S) \tag{11}$$

$S$ is a total internal dye-sensitized surface area.

$$p = \frac{\text{Vol} - N(4/3)\pi r^3}{\text{Vol}} \tag{12}$$

Porosity $p$ states the ratio of the volume that is not covered by photoanode particles to the total volume Vol.

$$CN = \text{-}10{,}29P + 10{,}22 \tag{13}$$

A linear relationship between $CN$ and $p$ [13]with $CN = 6$ fot $p = 0{,}41$ and $CN = 2{,}5$ for $p = 0{,}75$. $\alpha$ directly proportional to $S$ [11] conjunction eq. (6)-(8)

$$\alpha \propto (1 - p)(p + 2{,}89) \tag{14}$$

Based on references [10] value $\alpha = 5 \times 10^3$ cm$^{-1}$ on $p = 0{,}41$, so that previously unknown factors can be found and eq. (14) become

$$\alpha = 2568(1 - p)(p + 2{,}89) \tag{15}$$

Furthermore, electron porosity influences the transport of electrons which depend on particle connectivity. Based on experimental results and modeling results, effects $p$ on the electron diffusion coefficient $D$ described [12].

$$D = a|p - p_c|^b \tag{16}$$

with constants $a$ and $b$, $p_c$ is critical porosity. If we associate it $D$ on semiconductor electron mobility $\mu$, basic charge $e$ and working temperature $T$, then we can make a variation of the electron mobility in the material ZnO (205–300 cm$^2$V/s), $TiO_2$ (0,1 – 4 cm$^2$V/s) [16], $Nb_2O_5$ (2,3 cm$^2$V/s) [17].

$$D = \frac{kT\mu}{e} \tag{17}$$

$J - V$ characteristics obtained by substitution eq. (15) to (4).

This paper using a constant overlap method for nanostructure modeling and variation on photoanode materials to describe $J - V$ characteristics. There are four simulation stages. First, Input contains internal parameters according to Table 1 and combined with variations of the parameter and photoanode semiconductor material. Second, Variation is the parameter that we want to know its effect on the $J - V$ characteristics and its efficiency. Third, Calculation starts by entering the simulation's internal parameters to eq. (4) (6) (7) combined with nanostructure constant overlap method eq. (15) (16) (17) to obtain $V_{OC}$, $J_{SC}$, $P_{max}$, dan $\eta$. Fourth, Output consists of some simulation data including $J - V$ characteristics graph and efficiency $\eta$ for each variation.

**TABLE 1**. Internal parameter for input

| Parameter | Value | References |
|---|---|---|
| Light intensity, $\boldsymbol{\Phi}$ (cm$^{-2}$s$^{-1}$) | 1,0 x $10^{17}$ | 910 |
| Electron lifetime, $\boldsymbol{\tau}$ (ms) | 10 | 10 |
| Ideality factor $\boldsymbol{m}$ | 4,5 | 9 10 |
| Operating temperature $\boldsymbol{T}$ (K) | 300 | 9 10 |

## RESULT AND DISCUSSION

Characteristic modeling $J - V$ did after validation with experimental results. After that, there is a match between the results of analytic modeling and experimental results; the model was applied to describe the characteristics of the DSSC. The following are the results of the analytic model validation of some experimental data.

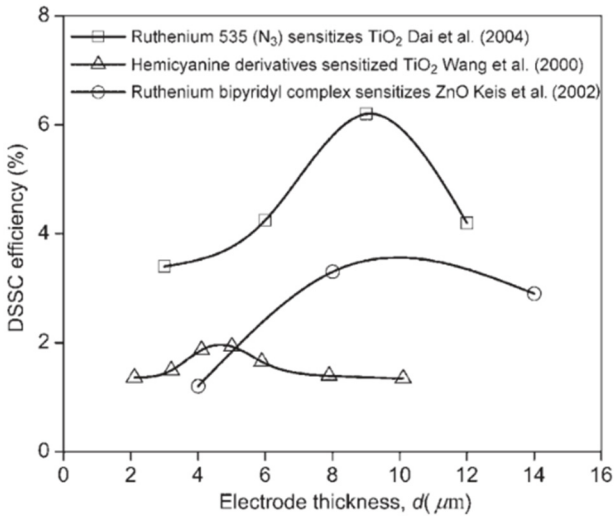


**FIGURE 2**. Relation of electrode thickness to DSSC efficiency

FIGURE 2 describes the effect of electrode thickness on the characteristics of DSSC current density. The picture above shows a graph of compatibility between experimental results and analytic models. DSSC performance using a photoanode Ruthenium bipyridyl complex sensitizer ZnO produces the highest efficiency at a thickness of 8 μm [18]. Furthermore, DSSC performance using Ruthenium 535 ($N_3$) photoanode sensitization of TiO2 by the sol-gel method at pH precursor 1.2 and temperature 250 ° C produces the highest efficiency at a thickness of 9 μm [19]. The third experimental result uses photo-method Hemicyanine derivatives sensitized $TiO_2$ produce the highest efficiency in 5 μm thickness [20].

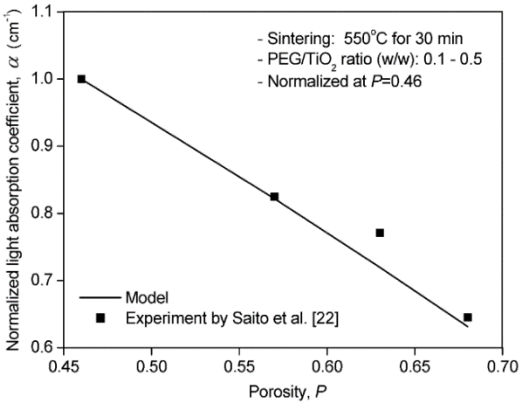


**FIGURE 3**. The relationship of porosity to the normalization of the absorption coefficient

Analytical porosity in eq. (14) and (15) affect the light absorption coefficient and electron diffusion coefficient. For this reason, it is necessary to validate the analytic model that describes the relationship between the two. The photoanode porosity was produced by sintering 550 ° C for 30 minutes with a PEG / $TiO_2$ ratio of 0.1 - 0.5 compared to the normalization of porosity of 0.46. FIGURE 3 describes the compatibility between experimental results and analytical models [11]. Porosity analytic modeling results illustrate the inverse relationship of the absorption coefficient; the greater the value of porosity actually reduce the absorption coefficient.

Moving on from the suitability of the results of the analytic model validation, further variations in photoanode semiconductors are needed. The following are the characteristics $J-V$ on photoanode with ZnO, $TiO_2$, $Nb_2O_5$ semiconductors.

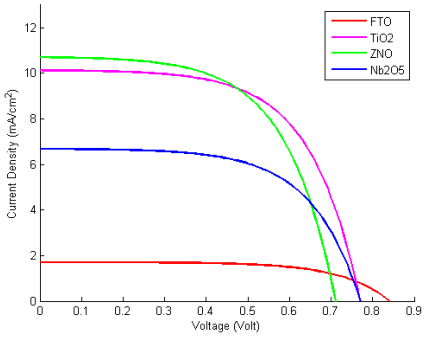


**FIGURE 4**. Photoanode semiconductors effect on $J-V$ characteristics.

There is a difference in the characteristics of $J-V$ in the variation of the photoanode semiconductor. Figure 4 describes the highest DSSC performance obtained in $TiO_2$ semiconductors, followed by ZnO, then Nb2O5. The superior performance of $TiO_2$ semiconductor photoanodes is inseparable from properties such as nanoparticle surface area and porosity. In addition to photoanodes based on TiO2, dye adsorption is high at 86 $m^2g^{-1}$, other factors such as particle boundaries, random electron trajectories support the effective transport of electrons (2016 - A critical). The surface area plays an important role in determining DSSC performance. The greater the surface area, the dye adsorption will also increase. Increased adsorption will increase current density so that efficiency increases. Although ZnO-based photoanodes have a higher electron mobility value and produce a greater current density than $TiO_2$. But the potential difference of the open circuit is still smaller than $TiO_2$. The anomaly can be explained in relation to the weak interaction process of dye molecules with semiconductor surfaces. The weak interaction process results in a low lifetime electron value so that electrons recombined more quickly with electrolytes. The high recombination rate decreases the potential difference when the circuit is open, even though the short circuit current value is high. The same is true for $Nb_2O_5$, which although it has a barrier layer to reduce electron recombination processes, but current density is small. As already explained that the surface area of a semiconductor has a large influence.

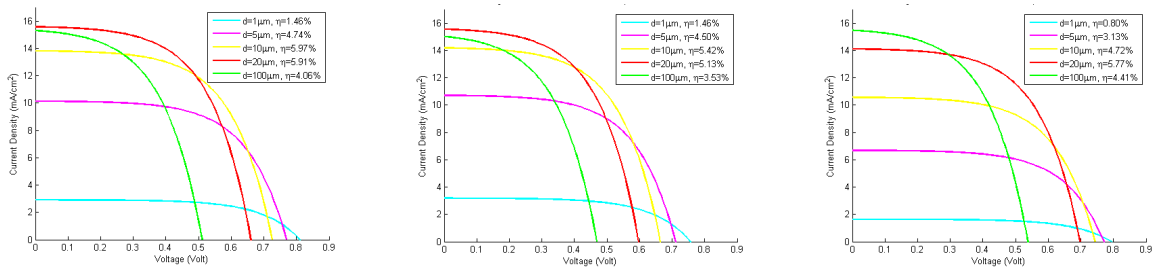


(a) (b) (c)

**FIGURE 5**. DSSC performance is influenced by photoanode thickness based on (a) $TiO_2$, (b) ZnO, (c)$Nb_2O_5$

After getting the DSSC performance sequence, then we will determine the optimum nanostructure parameters. These parameters include thickness, absorption coefficient, diffusion coefficient, and porosity according to analytic modeling. The nanostructural parameters are obtained by the total differential method to determine the optimum thickness. Other parameters are considered constant when the thickness of the photoanode is varied. FIGURE 5 showed the greatest efficiency in $TiO_2$ and ZnO occurred at a thickness of 10 µm while $Nb_2O_5$ at 20 µm. There is a pattern of a drastic increase in current density along with an increase in the thickness of the photoanode, but after reaching the peak, it will slowly decrease. This is explained by the photogeneration process. The thicker the photoanode will increase the surface area for the interaction of dye molecules. The thicker, the more photons can be absorbed. The light penetration depth limits the amount of current density. Even the thicker the photoanode will actually increase the recombination rate. Both of these will increase the number of electrons lost and reduce current density. After obtaining the optimum thickness, the value will be used as a reference to determine the absorption coefficient parameters.

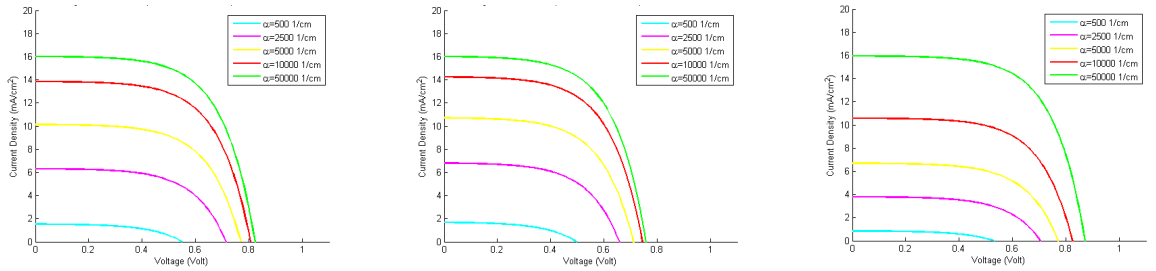


(a) (b) (c)

**FIGURE 6**. DSSC performance is influenced by the photoanode absorption coefficient based on (a) $TiO_2$, (b) ZnO, (c) $Nb_2O_5$

The absorption coefficient affects the performance of DSSC, as in FIGURE 6. The greater the absorption coefficient value states, the greater the current density and potential difference. The linear relationship can be explained that the greater the absorption coefficient, the more photons can be absorbed by the dye molecule on the surface of the photoanode. As a result, more electrons are produced and increase efficiency. This result is according to eq. (15) where the absorption coefficient is influenced by photoanode porosity. But before discussing porosity, we will review the diffusion coefficient.

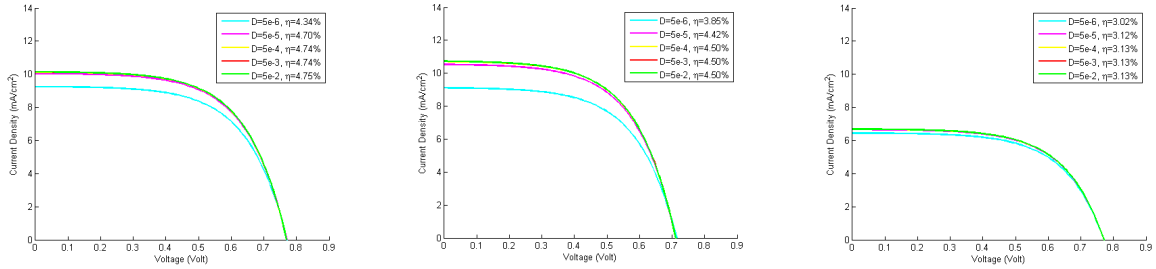


(a) (b) (c)

**FIGURE 7**. DSSC performance is influenced by photoanode diffusion coefficients based on (a) $TiO_2$, (b) ZnO, (c) $Nb_2O_5$

The effect of the diffusion coefficient on DSSC performance is stated in FIGURE 7. The diffusion coefficient has a proportional relationship with the current density, but vice versa for its voltage. This is because increasing the value of the diffusion coefficient increases the increase in electron diffusion length. This means that the greater the diffusion coefficient, the recombination process decreases, and the more electrons can be harvested. This increases current density. But the greater the electron extraction indicates the smaller the electron density value. The small electron density decreases the potential difference value. In addition, the diffusion coefficient depends on electron mobility. As discussed earlier in experimental detail, the sequence of electron mobility is from the largest to the smallest in a row ZnO, $TiO_2$, then $Nb_2O_5$. Therefore, the results of analytical modeling also show results that are not much different. After discussing the thickness parameters, absorption coefficient, and diffusion coefficient, we then discuss porosity.

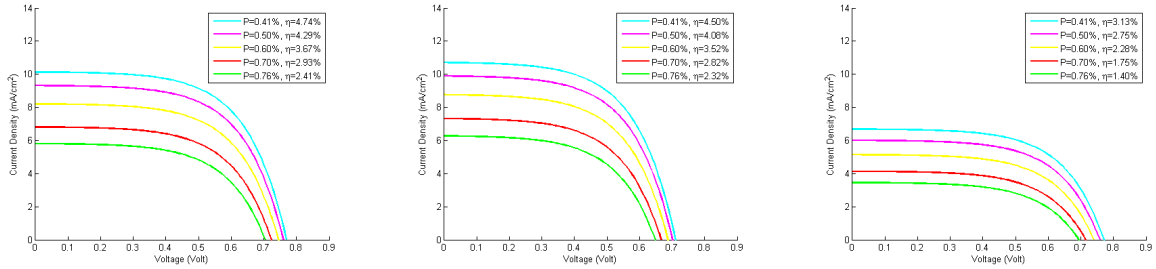


(a) (b) (c)

**FIGURE 8**. DSSC performance is influenced by photoanode porosity based on (a) $TiO_2$, (b) ZnO, (c) $Nb_2O_5$

Porosity plays a no less important role with the photoanode surface area in influencing DSSC performance. FIGURE 8 shows that the greater the porosity value of a photoanode will decrease the magnitude of the current density and the potential difference produced. This is related to the absorption coefficient and the diffusion coefficient. According to eq. (15) and (16) where the greater the absorption coefficient value and the diffusion coefficient actually decreases the porosity value. In other words, the smaller the porosity, the higher the internal surface area so that it will improve the performance of DSSC.

## CONCLUSION

Analytic modeling using the constant overlap method is used for the optimization of DSSC nanostructural parameters. Before the modeling was applied, validation was carried out with experimental results. There is a match on the effect of thickness and photoanode absorption coefficient as a result of modeling and experimental results. The results of modeling with semiconductor variations in photoanodes show that $TiO_2$ is the optimal material when compared to ZnO and $Nb_2O_5$. Photoanode surface area, electron mobility, and surface and dye interactions that affect this. Nanostructure optimization has been done by analytic modeling to obtain optimum parameters for $TiO_2$ and ZnO thickness at 10 μm and $Nb_2O_5$ at 20 μm. The optimum porosity parameters at 0.41 on all photoanode. Whereas the parameters of the absorption coefficient and diffusion coefficient have a comparable relationship to the performance of DSSC. This model can be used for further research on solid-state DSSC.

## ACKNOWLEDGMENTS

This work is funded by a master's thesis research program with a research contract number 1833/UN25.3.1/LT /2019 Monday, March 18 of the 2019 budget year.

## REFERENCES

1. NOAA. CO2 Trend. (2019).
2. Raj, C. C. & Prasanth, R. A critical review of recent developments in nanomaterials for photoelectrodes in dye-sensitized solar cells. J. Power Sources 317, 120–132 (2016).
3. Xu, T. Nanoarchitectured Electrodes for Enhanced Electron Transport in Dye-Sensitized Solar Cells. 217–298 (2011). doi:10.1007/978-0-85729-638-2
4. Yeoh, M. Recent advances in photo-anode for dye-sensitized solar cells : a review. (2017). doi:10.1002/er.3764
5. Supriyanto, E. Pengaruh Thermal Annealing terhadap Struktur Kristal dan Morfologi Bubuk Titanium Dioksida (TiO2) The Thermal Annealing Effect on Crystal Structure and Morphology of Titanium Dioxide (TiO2) Powder. 15, 37–41 (2014).
6. Vittal, R. Zinc oxide based dye-sensitized solar cells: A review. Renew. Sustain. Energy Rev. 70, 920–935 (2017).
7. Tayyan, A. A. El. Dye-sensitized solar cell: parameters calculation and model integration. J. Electron Devices 11, 616–624 (2011).
8. Soedergren, S. Theoretical Models for the Action Spectrum and the Current-Voltage Characteristics of Microporous Semiconductor Films in Photoelectrochemical Cells. J. Phys. Chem. 98, 5552–5556 (1994).
9. Lee, J.-J. Current Density versus Potential Characteristics of Dye-Sensitized Nanostructured Semiconductor Photoelectrodes. 2. Simulations. J. Phys. Chem. B 108, 5282–5293 (2004).
10. Gómez, R. Photovoltage dependence on film thickness and type of illumination in nanoporous thin film electrodes according to a simple diffusion model. Sol. Energy Mater. Sol. Cells 88, 377–388 (2005).
11. Saito, Y. Morphology control of mesoporous TiO2 nanocrystalline films for performance of dye-sensitized solar cells. Sol. Energy Mater. Sol. Cells 83, 1–13 (2004).
12. Benkstein, K. D. Influence of the Percolation Network Geometry on Electron Transport in Dye-Sensitized Titanium Dioxide Solar Cells. J. Phys. Chem. B 107, 7759–7767 (2003).
13. Van de Lagemaat, J. Nonthermalized electron transport in dye-sensitized nanocrystalline TiO2 films: Transient photocurrent and random-walk modeling studies. J. Phys. Chem. B 105, 11194–11205 (2001).
14. Nanko, M. Surface self-diffusivity of under high-pressure gas. Phys. Rev. B - Condens. Matter Mater. Phys. 56, 6965–6969 (1997).

15. Ni, M. Theoretical modeling of TiO2/TCO interfacial effect on dye-sensitized solar cell performance. Sol. Energy Mater. Sol. Cells 90, 2000–2009 (2006).
16. Zhang, Q. ZnO nanostructures for dye-sensitized solar cells. Adv. Mater. 21, 4087–4108 (2009).
17. Song, J. A crystallographic study of Nb2O5 .3WO 3. Acta Crystallogr. 17, 454–454 (2016).
18. Keis, K. A 5% efficient photoelectrochemical solar cell based on nanostructured ZnO electrodes. 73, 51–58 (2002).
19. Dai, S. Dye-sensitized solar cells, from cell to module. Sol. Energy Mater. Sol. Cells 84, 125–133 (2004).
20. Wang, Z. Photoelectric Conversion Properties of Nanocrystalline TiO2 Electrodes Sensitized with Hemicyanine Derivatives. 9676–9682 (2000).